Steady State and Transient Modelling of A Three-Core Once-Through Steam Generator

Håvard Falch, **Geir Skaugen**

SINTEF Energy Research, Sem Sælands vei 11, Trondheim, Norway
Corresponding author: haavard.falch@sintef.no

Abstract: To reduce emissions and save fuel in offshore power production using gas turbines, one can use the gas turbine exhaust as a heat source for a bottoming cycle for heat and power production. This can replace about one in four gas turbines. In offshore applications weight and size become more important and thus a once-through steam generator (OTSG) is a way to achieve low weight for the bottoming cycle. To reduce the size and weight of the OTSG further, one can reduce the tube diameter in the tube bundles. In this work a three-core OTSG, representing the economizer, evaporator, and superheater, was modelled and the design optimized to achieve minimum weight, while producing a certain amount of power and keeping within constraints of flue gas and steam pressure losses. This was done for varying tube diameters in each of the cores, in steady state. Afterwards transient simulations were performed for each optimized design to find their response times to a step change in the gas turbine load. The evaporator has the biggest impact on both the weight and the response time, while the superheater and economizer had similar and smaller impacts on both the weight and response time.

Keywords: Heat exchanger, OTSG, power production, steam production, optimization, transient modelling

1. INTRODUCTION

In offshore oil and gas production a large source of CO_2 emissions is gas turbine exhaust, and in 2023 it accounted for 80% of CO_2 emissions from Norwegian oil and gas production according to the Norwegian Petroleum Directorate (2023). One opportunity for reducing these emissions is to install a steam bottoming cycle to use the hot exhaust gas as a heat source. By installing a bottoming cycle, the fuel consumption of a gas turbine can be reduced by about 25% (Nord and Bolland, 2012; Mazzetti et al.. 2014). For a processing facility with a fleet of several gas turbines, installing a bottoming cycle will mean that one or more of the gas turbines can be removed. In the bottoming cycle, illustrated in Fig. 1, pressurized water is heated, evaporated, and superheated through a heat recovery steam generator (HRSG) and then expanded in a steam turbine to generate power. The low-pressure steam is condensed and cooled by sea water before being pumped back to the HRSG. Other non-conventional fluids have also been studied for use in bottoming cycles, including air by Pierobon and Haglind (2014), CO2 by Walnum et al. (2013) and Skaugen et al. (2014), and organic Rankine cycles by Pierobon et al. (2014) and Motamed and Nord (2022). However, only steam bottoming cycles have been installed on the Norwegian Continental Shelf, making it the most mature technology. The HRSG is a large installation with a weight that can reach several hundred tons, so, for offshore installation a compact bottoming cycle will be necessary. This can be achieved by optimizing the HRSG. In offshore installations, the HRSG without a steam drum will normally be suggested and the excess heat is recovered in a once-through steam generator (OTSG). In (Mazzetti et al., 2021) an outline on how a compact steam bottoming cycle can be designed is discussed - where one of the main size/weight drivers was the tube diameter selection in the OTSG. Similar analysis was shown by Montañés et al. (2023) for a compact steam bottoming cycle for heat and power production on a floating production plant. Deng et al. (2021) studied vibrations of the tubes in an OTSG and found that vibrational constraints increased the optimal weight of the OTSG, and that the increase was larger for the single-core case compared to the three-core case.

In this work a three-core OTSG is studied in detail in order to optimize the tube diameters and circuiting in the three cores, the economizer, the evaporator, and the superheater, individually, in order to find the minimum weight for a specified duty and with restriction on pressure losses. In earlier works optimizing OTSG designs, the tube diameter has been used as an optimization parameter in the single-core case and fixed in the three-core case. However, in this work, we investigate four different industry standard tube diameters to get a thorough understanding of how each part of the OTSG is affected by changing the diameter of the tube and if having different diameters

⋆ This publication has been produced with support from the LowEmission Research Centre (www.lowemission.no), performed under the Norwegian research program PETROSENTER. The authors acknowledge the industry partners in LowEmission for their contributions and the Research Council of Norway (296207).

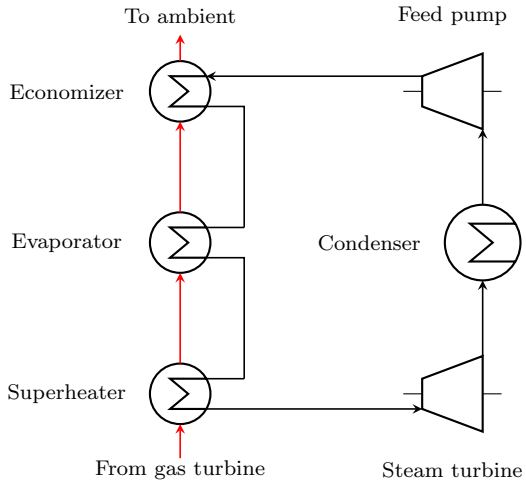

Fig. 1. Heat recovery steam generation from gas turbine exhaust in a bottoming cycle for power production.

in each of the cores will be optimal. This is done by optimizing each core with respect to weight and afterwards looking at the response time for a load change.

2. NUMERICAL METHODS

To optimize the geometry of the OTSG and perform dynamic simulations we used an in-house modeling tool developed by SINTEF Energy Research (Skaugen et al., 2013). The OTSG geometry optimization was done in several steps. First, a thermodynamic optimization of the whole bottoming cycle was done to investigate the potential power production and find a suitable mass flow and pressure for the geometric optimization. After this, the geometric optimization of the three cores was performed in three steps. From the thermodynamic optimization, we knew the mass flow and the pressure of the steam at the superheater outlet which coincides with the exhaust inlet, both of which are at the bottom of the superheater. Thus, we began with the superheater optimization, and using the lowest weight design we used the flow conditions from the top of the superheater to optimize the evaporator and again using the flow conditions from the lightest evaporator design we optimized the economizer.

2.1 Thermodynamic optimization

The thermodynamic optimization considers the entire bottoming cycle including the OTSG at a flowsheet level, as seen in Fig. 1, however, it does not include the full OTSG geometry. To solve the model it takes both external and process variables. The external variables are the mass flow, pressure, and composition of the exhaust gas coming from the gas turbine and a pinch point temperature difference (PPTD), i.e. the minimum temperature difference between the exhaust gas and the water. The process variables are the outlet temperature of the exhaust gas, the water pressure at the pump outlet, the water temperature at the turbine inlet, the water pressure at the turbine outlet, and the temperature increase of the cooling water in the condenser. The heat transferred from the exhaust gas to the water Q is calculated as

$$Q = (h(p,T)_{\text{ex,in}} - h(p,T)_{\text{ex,out}})\dot{m}_{\text{ex}}, \tag{1}$$

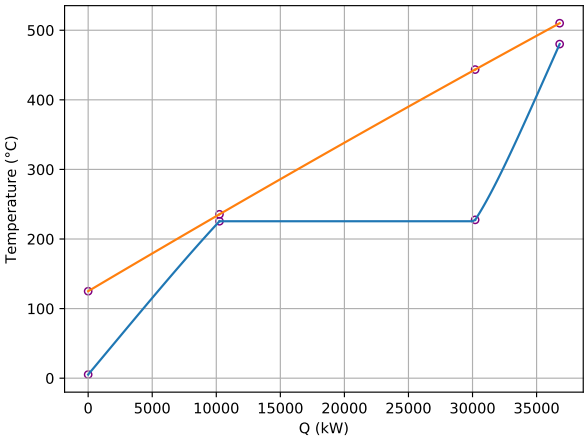

Fig. 2. Typical temperature profile in a counter flow heat exchanger as a function of the heat transferred along the flow direction of the cold fluid. The pinch point, where the temperature of the cold and the hot liquids are the closest, is here marked by the second set of dots and is 10°C.

where h is the enthalpy, p the pressure, T the temperature, and $\dot{m}$ is the mass flow rate, while the subscript ex denotes the exhaust and the subscripts in and out refer to the inlet and outlet states of the OTSG. This heat transfer is then used to calculate the water flow rate $\dot{m}_{\text{w}}$ as

$$\dot{m}_{\text{w}} = \frac{Q}{(h(p,T)_{\text{w,out}} - h(p,T)_{\text{w,in}})}. \tag{2}$$

The amount of power produced in the turbine expansion W_{exp} is calculated from an isentropic expansion with isentropic efficiency 0.85, while the pump work W_{pump} is calculated from an isentropic compression with efficiency 0.7. Together these give the net power produced by the bottoming cycle W_{net} as

$$W_{\text{net}} = W_{\text{exp}} - W_{\text{pump}}. \tag{3}$$

The optimization is performed using the gradient-based constrained optimization solver NLPQL by Schittkowski (1986) to optimize the process variables with the objective of maximizing the net power produced. The optimization variables are all given initial values as well as lower and upper bounds when passed to NLPQL. Instead of optimizing all the parameters one or more can also be given a fixed value. In addition, it is subject to several constraints, such as a minimum vapour fraction at the steam turbine outlet and minimum pinch temperature, which are all inequality constraints, and an equality constraint to ensure continuous pressure for the water. In our case, we fix the water temperature at the turbine inlet and then the pinch is at the onset of boiling of the water, and thus the PPTD decides the temperature difference between the exhaust and water at this point. This can be seen as the second set of points in Fig. 2 which shows standard temperature profiles of the exhaust (above) and water (below) as a function of heat transferred in the OTSG.

2.2 Geometric optimization

The geometry of the OTSG is described by three cores, the economizer, evaporator, and superheater, each consisting

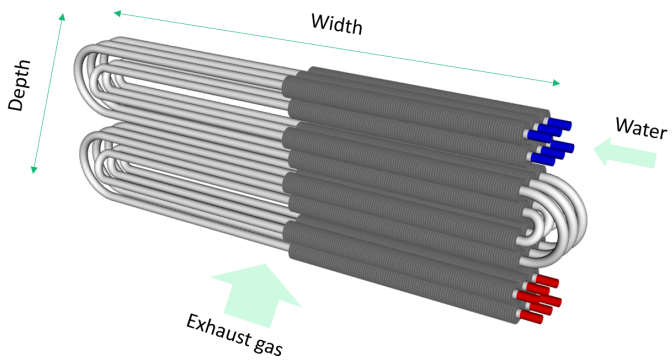

Fig. 3. A simple tube bundle, the fins are only shown for half of the width to get a better view of the tubes.

of a tube bundle along with support beams, as well as a surrounding duct for each tube bundle to contain the exhaust gas and an inlet duct for the superheater and an exit duct for the economizer. The duct size and thus weight is dependent on the size of the tube bundles. The weight of the entire core consists of the tube bundle weight, as well as the duct surrounding the bundle and the inlet or exit duct when applicable. A simple example tube bundle is shown in Fig. 3. We see that each tube passes through 4 times, i.e. 4 passes, there are 2 parallel rows of tubes in each pass, i.e. 2 rows per pass, and there are 3 tubes per row. The width of the tube bundle equals the length of the water flow in one row, the depth is the length of flow for the exhaust gas along the tube bundle. The tubes are laid out with a 30° offset between each row which gives a hexagonal pattern. In addition, the tubes have fins on the outside to improve the heat transfer from the exhaust gas. The fins have a set thickness, but the distance between them and their height can be varied.

To solve each of the cores we start by assuming that all tubes in one row are equal to get a 2D problem and then discretizing along the width and depth such that each tube is divided in several tube segments, or nodes, and the exhaust gas flows in several separate columns. This allows us to start from the outlet of the bottom tube and solve the heat transfer for each node. The heat transfer Q is given by

$$Q = UA\Delta T, \tag{4}$$

where U is the overall heat transfer coefficient, A is the heat transfer area and $\Delta T = T_{\text{ex}} - T_{\text{w}}$ is the temperature difference between the exhaust gas and water. In the simplest case one can use the initial temperature difference as ΔT. However, in the OTSG there is quite a big temperature change in each node and thus we instead use Heun's method to update the temperature difference with intermediate steps and thus get a better heat transfer calculation. The heat transferred is then used to update the fluid enthalpies as

$$h_{\text{out}} = h_{\text{in}} - \frac{Q}{\dot{m}}, \tag{5}$$

where both the exhaust and the water get a minus sign as we are calculating backwards along the water. Each node is solved iteratively until the end of the tube pass and then the tube above is solved in the same fashion and so on until one reaches the inlet. As the pressure and enthalpy of the water might vary for parallel passes, they are here mixed to get a common outlet condition and the same is also done for the exhaust gas. The outlet conditions can then be used as inlet conditions for the next core.

Table 1. Variables with initial guess and bounds for the geometric optimization.

Variable	Unit	Initial guess	Range
Tubes per row	[ ]	50	5-180
Transversal fin tip gap	[mm]	50	5-125
Fin height	[mm]	6.5	5-20
Fin pitch	[mm]	5.5	2-8

Just as for the thermodynamic optimization we also use NLPQL for gradient-based constrained optimization of the core geometry. The objective of the optimization is to minimize the total weight of the core. The variables with initial values as well as their range are shown in Table 1. The constraints consist of a single equality constraint for the heat recovered as well as inequality constraints for pressure losses for both fluids, maximum exhaust velocity, and minimum fin and tube spacing. There are also a few variables that NLPQL does not optimize, namely the number of passes, the number of tubes per row, the width of the core, and the diameter of the tubes. These are given as inputs and the NLPQL optimization is run a separate time for each combination. The number of passes and tubes per row are both integer values and thus not suited for NLPQL to optimize. The width is also controlled separately to ensure that all three cores have the same width. Finally, the tube diameter is given certain fixed values based on industry-standard tubes.

After the thermodynamic optimization, we have the heat transferred in each core, the mass flow of the water, as well as the temperature and pressure at the steam turbine inlet and thus the superheater outlet. With these values as well as the mass flow, temperature, and pressure of the exhaust gas we can begin with optimizing the superheater. After finding the lightest superheater design, we can use the inlet conditions of the superheater as the outlet conditions of the evaporator and optimize it, and finally we can do the same with the economizer after optimizing the evaporator.

As we calculate the heat transfer and pressure drop at each node, we need correlations for both suitable for our geometry. For the heat transfer and pressure loss of the exhaust we use the ESCOA correlation (Ganapathy, 2002). For the water/steam inside the tubes the heat transfer coefficient is calculated from the Gnielinski (1976) correlation for single phase flow and the Bennett and Chen (1980) correlation during evaporation. The pressure losses are calculated with the Blasius correlation for single phase flow and the Friedel (1979) correlation during evaporation. To calculate the thermodynamic properties of the water the IAPWS formulation is used (Wagner and Pruß, 2002), while the cubic Peng-Robinson equation of state from Thermopack (Wilhelmsen et al., 2017) is used for the exhaust gas.

2.3 Transient modelling

The transient model uses many of the same principles as the steady state optimization. We assume equal conditions for all tubes in a row, so we only need to solve for one and we discretize each bundle along its width and depth.

However, in contrast to the steady state model, we use as input the exhaust entering the bottom of the superheater and the water entering the top of the economizer. In addition, we also calculate the wall temperature for each node, such that the heat transfer is calculated using Eq. 4 between the wall and each fluid separately, and conductive heat transfer along the wall is included. This means that the wall interacts with the two fluids and the temperature change ΔT_{wall} in the wall is given by

$$\Delta T_{\text{wall}} = \frac{Q_{\text{ex}} - Q_{\text{w}} + Q_{\text{cond}}}{C_p}, \tag{6}$$

where Q_{ex} is the heat transferred from the exhaust to the wall and Q_{w} is the heat transferred from the wall to the water, both of which are usually positive, Q_{cond} is the net conductive heat transfer along the tube wall, and C_p is the combined heat capacity of the wall and fins at the temperature of the wall.

To start the transient modeling we first specify the temperature of each wall node and we then solve along each fluid flow. For the water we start from the inlet of the economizer, and for each node we calculate the heat transferred from the wall at that node to the water as well as the pressure loss of the water. This is then done all the way through until the end of the economizer which gives the inlet conditions for the water entering the evaporator. The same procedure is applied to the evaporator and superheater. For the exhaust gas we start from the exhaust gas inlet at the bottom of the superheater. Along each exhaust gas column, we calculate the heat transferred to the wall at that node as well as the pressure loss, then move to the next node above and so on until leaving the top of the economizer. Calculating the conductive heat transfer for each wall node allows us to use Eq. 6 and the time step to update all wall temperatures. This constitutes a single step in the time integration and this procedure is repeated until the chosen finish time of the integration. To ensure each time step is of a sufficient length the fourth-order Runge-Kutta-Fehlberg algorithm from GSL (Galassi et al., 2009) is used. In addition, during the integration, the inlet conditions of the water and exhaust gas, i.e. pressure, temperature, and composition or gas turbine load, can be changed freely at any specified time.

3. RESULTS

3.1 Thermodynamic results

We first consider the simplified case of a heat exchanger without geometry, where the heat recovered and net power is calculated for varying values of the PPTD. For all the simulations the exhaust gas is assumed to come from a LM2500+G4 gas turbine running at 90% load, giving an exhaust inlet temperature at 510.1°C, pressure of 1bar and a mass flow of 86.12kg/s unless otherwise specified and we fix the outlet steam temperature to 480.1°C. The optimization was performed with PPTDs ranging from 0 to 30°C to give a good grasp on how the PPTD affects the power produced and the heat recovered. At a PPTD of 30°C we have pinch at both the onset of boiling and the water outlet and going lower than this we would only have pinch in the hot end. Having pinch in only the hot end would lead to a lower mass flow and less power

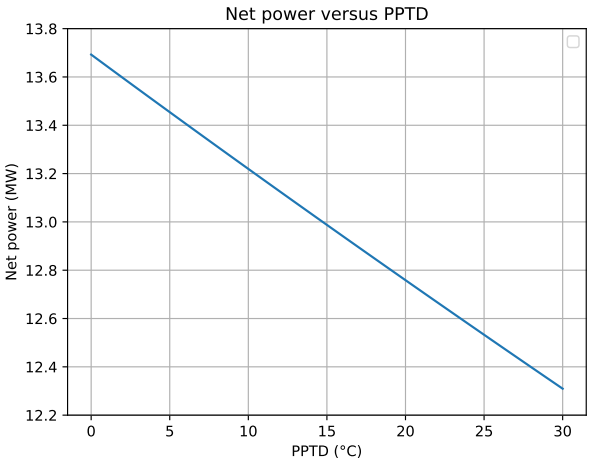

Fig. 4. Net power produced in the combined cycle OTSG without geometry for varying PPTD for fixed outlet temperature 480.1°C.

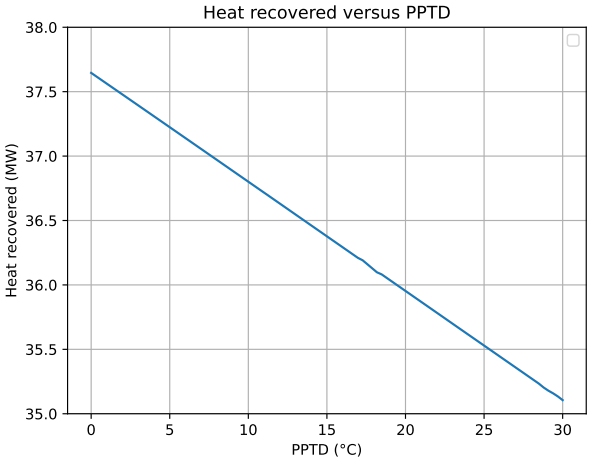

Fig. 5. Heat recovered in the OTSG without geometry for varying PPTD for fixed outlet temperature of 480.1°C.

produced and has not been investigated here. The net power produced is shown in Fig. 4 and the heat recovered from the exhaust gas is shown in Fig. 5. We see that the amount of heat recovered is larger than the net power produced by a factor of almost 3, with a maximum power produced of 13.7MW and a maximum heat recovered of 37.6MW, and that both decrease linearly with an increase in the PPTD. Thus, we want the PPTD to be as small as possible, but this does not take into account the size of the heat exchanger and the pressure loss in the heat exchanger. When the PPTD becomes smaller the necessary area increases and thus at a very small PPTD the OTSG needs to be very large. As obtaining a PPTD close to 0 is very hard we will use the flow conditions calculated for a PPTD of 10°C to optimize the geometries of the separate cores of the heat exchanger. The flow conditions are given in Table 2, and it also contains the heat duties used for the optimization where some extra duty is moved from the economizer to the evaporator.

Table 2. Input values for the water and exhaust gas stream for the geometric optimization.

Variable	Unit	Value
Inlet temperature of exhaust gas	[C]	510.1
Outlet temperature of steam	[C]	480.1
Inlet pressure of exhaust gas	[bar]	1
Outlet pressure of steam	[bar]	25.74
Mass flow of exhaust gas	[kg/s]	86.12
Mass flow of steam	[kg/s]	10.846
Superheater heat duty	[MW]	6.2
Evaporator heat duty	[MW]	23.0
Economizer heat duty	[MW]	6.2

3.2 Geometric results

Based on the flow conditions in Table 2 found in the thermodynamic optimization we performed the geometric optimization. The heat loads used are also given in the table, but they are slightly different from the thermodynamic optimization. In Fig 2 we see three distinct phases for the water, between the first and second pairs of dots it is heated, then, between the second and the third it boils and between the third and the fourth it is superheated. This corresponds to the economizer, evaporator, and superheater. However, for the geometric optimization we move some extra heat duty to the evaporator from the economizer to ensure that we avoid boiling in the economizer for different part loads. This could lead to instabilities such as the Ledinegg instability (Ledinegg, 1938) which we want to avoid. The pressure loss restriction was set to 600Pa for the exhaust in each core to get a total pressure drop of less than 3000Pa when including the inlet and exit transition ducts. The water pressure loss restriction was set to 100000Pa or 1bar in the evaporator and superheater and to 50000Pa in the economizer as here there is only liquid water which has a lower pressure loss. As lower tube diameters increase pressure losses it can become favourable to have many rows per pass when optimizing with respect to weight. However, this can become quite complicated to manufacture. Therefore we locked the number of rows per pass to be 2 in the evaporator and superheater where we have boiling and steam and thus higher pressure losses, and the number of rows per pass to 1 in the economizer as it has a lower pressure loss.

The weight of each of the cores, including both the tube bundle and ducting, and inlet duct for the superheater and outlet duct for the economizer, were optimized with widths varying from 3m to 7m with 0.5m intervals. For each width the design with the number of passes which gave the lightest weight were used as the input to the next core, i.e. from superheater to evaporator and evaporator to economizer. The investigated tube diameters are shown in Table 3 and are the tube diameters labeled as sensible range for offshore systems by Montañés et al. (2021) based on the ASME standard (STEELTUBE, 2021).

To investigate the weight savings of having different tube diameters in different cores we also consider cases where not all three cores have the same tube diameter. However, with the four tube diameters from Table 3 there are a total of 60 such combinations. Thus, we need to reduce this further. To begin with we notice that in the economizer there only flows liquid water, in the superheater there is only steam, while the evaporator has a mix. This means that we expect the pressure loss to be largest in the superheater and smallest in the economizer. In addition, the superheater is closest to the gas turbine so it experiences the harshest exhaust gas conditions while the economizer which is furthest away experiences the least harsh exhaust gas conditions. Thus, we expect that the superheater should be made of the sturdiest and largest tubes. Because of these two reasons we only consider combinations where the tube diameter does not increase when moving from the superheater to evaporator or evaporator to economizer, however, two or three of the cores can have the same diameter. In addition, we expect an actual design to not have huge differences in the tube diameters and thus we only consider designs where the change in tube outer diameter from one core to the next is at most 6.35mm or $^1/_4''$. Including the designs where the tube diameter is equal in all three cores leaves us with the designs consisting of the combinations shown in Table 4.

Table 3. The different tubes with inner and outer diameter that were investigated in this study.

Inner diameter [mm]	Outer diameter [mm]	Outer diameter
32.56	38.1	1 ½″
27.53	31.75	1 ¼″
21.18	25.4	1″
15.75	19.05	¾″

Table 4. The different combinations of inner diameters in the superheater, evaporator and economizer that were optimized for minimal weight.

Superheater [mm]	Evaporator [mm]	Economizer [mm]
32.56	32.56	32.56
32.56	32.56	27.53
32.56	27.53	27.53
27.53	27.53	27.53
32.56	27.53	21.18
27.53	27.53	21.18
27.53	21.18	21.18
21.18	21.18	21.18
27.53	21.18	15.75
21.18	21.18	15.75
21.18	15.75	15.75
15.75	15.75	15.75

The optimized weights as a function of width for each of the cores in the OTSG for the tube diameter combinations given in Table 4 are shown in Fig. 6, where repeating combinations are excluded for the superheater and evaporator. For both the evaporator and the economizer we note that the weight has a very weak dependence on the previous core(s) and almost only depends on the tube diameter in that core. This is due to the fact that we fix the heat transfer in the previous cores and the pressure loss is relatively small in the evaporator and restricted in the superheater, leading to very similar conditions for the core independent of the geometry of the previous ones. However, for larger superheater diameters the pressure loss does not reach the maximum and thus we see a slightly lower weight of the evaporator as the water has a lower pressure and thus also a lower evaporating temperature. We also observe that reducing the tube diameter always leads to a weight reduction for the evaporator, the economizer and the total OTSG, and sometimes for the superheater. The reason

for this is that a smaller tube diameter gives more heat transfer area per volume which improves the overall heat transfer and thus less weight is needed. However, the smaller tubes also give a larger pressure drop in the tubes. In the superheater there is only steam flowing inside the tubes which leads to a pretty high pressure loss. As this pressure loss is restricted this leads to significantly more tubes per row being needed for smaller tube diameters to reduce the flow in each tube and thus the pressure loss, which counteracts the weight saving of having smaller tubes. Thus, we see that for a tube diameter of 21.18mm there is only a weight saving for widths up to 5m compared to the larger diameter, while for 15.75mm there is only a weight saving up to a width of 3.5m. In addition, this larger pressure drop for smaller diameters leads to the optimal width becoming smaller such that the length of each tube is shorter which also helps reduce the pressure loss. In the evaporator and economizer the pressure loss is not close to the restriction and thus we do not see the same effect in either of them.

If we compare the weight savings in each of the cores we see that in the superheater and economizer we only save about 9 and 8.5 tons respectively changing from the largest to the smallest tube diameter, while we save about 50 tons in the evaporator. As the evaporator transfers a lot more heat than the other two cores it is heavier and there is more to save by reducing the evaporator tube diameter. Finally, the total weight of the OTSG shows the same trend as each of the cores, with a noticeable weight reduction for each tube diameter. There are also four bands where the weights are relatively close, one for each evaporator diameter, which shows that reducing the evaporator diameter has the biggest effect on the weight of the entire OTSG.

3.3 Transient results

While the weight of the OTSG is very important for their use offshore, reducing the diameter of the tubes also changes the dynamic response of the OTSG. This is due to the fact that when reducing the tube diameter we get more heat exchanger area per volume of flow and per mass of the tubes. This means that we both reduce the amount of water stored inside the OTSG tubes and the mass of the tubes which reduces the total heat capacity of the system. This means that we expect faster response times for the designs with smaller tube diameters, however, we need to check how much each different core affects the response time. To do this we did a simple transient test. The OTSG was initialized with the flow values used for the steady state optimization and ran for a sufficiently long time such that it was in steady state. Then the gas turbine load was changed instantaneously from 90% to 50%, which amounts to a change in the exhaust gas temperature from 510.1°C to 510°C and a change in exhaust gas mass flow from 86.12kg/s to 66.34kg/s. This was then run until a new steady state and we found the time for the water outlet temperature from the superheater to reach within 1% and 0.1% of the new steady state value. The resulting times are shown in Table 5.

Looking at the response times we see that just like the weights of the OTSG the response time is generally reduced for reduced diameters, with some slight increases for a few cases, which could be due to the width only being optimized in discrete steps. Changing from the heaviest design with the largest tube diameters to the lightest design with the smallest tube diameters halves the response time. Also, the reduction is not evenly distributed between the cores, instead, the evaporator clearly has the biggest impact. This is again due to the evaporator being significantly heavier and thus also having significantly more thermal mass in the tube bundle which takes longer to cool. The reduction in response time is very similar when reducing the diameter of the economizer and of the superheater, which is because of their weight saving, and thus the thermal mass reduction is approximately the same. Finally, we note that the response time is changed more for larger tube diameters. For example, reducing the evaporator diameter from 32.56mm to 27.53mm reduces the 1% response time by about 1900s while changing from an evaporator diameter of 21.18mm to one of 15.75mm only reduces the response time by about 1200s. However, if we look at the percentage-wise reduction this is about a 20% reduction for both cases. For comparison reducing the superheater diameter gives a reduction of -0.8%-2.2% and the economizer 0.3%-2.4% when ignoring the outlier with 21.18mm diameter in all three cores. Compared with the evaporator the relative change is significantly smaller for the response time contribution of the economizer and the evaporator compared to the weight savings, showing that the evaporator is significantly more important for the response time. This could also explain why the response time of the design with 21.18mm tube diameter in all three cores has a significant increase in response time compared to the designs with similar diameters. In this case, the superheater weight increases quickly with the diameter, leading to an optimal width smaller than the design with a larger superheater diameter. Thus, the evaporator becomes heavier and as it contributes more to the response time than the other cores compared to its weight this then leads to an increase in the response time.

4. CONCLUSION

In this study, a numerical framework has been used to minimize the weight of an OTSG consisting of three cores for varying tube diameters in each of the cores. First, the OTSG combined cycle was investigated without a geometric heat exchanger to find suitable operating conditions. The chosen operating conditions were then used to minimize the weight of each of the three cores in the OTSG. It was found that the evaporator was the heaviest and thus had the largest weight savings when reducing the tube diameter, while the superheater had diminishing weight savings due to higher pressure losses for steam in smaller tubes. Finally, the transient response for each of the optimal designs was investigated when reducing the exhaust gas flow rate and keeping the water flow rate constant. Here it was found that reducing the tube diameter and thus the weight generally reduced the response time of the OTSG due to reducing the thermal mass of the system. Just as for the weight the evaporator had clearly the biggest effect due to it having the largest thermal mass reduction when reducing the tube diameter.

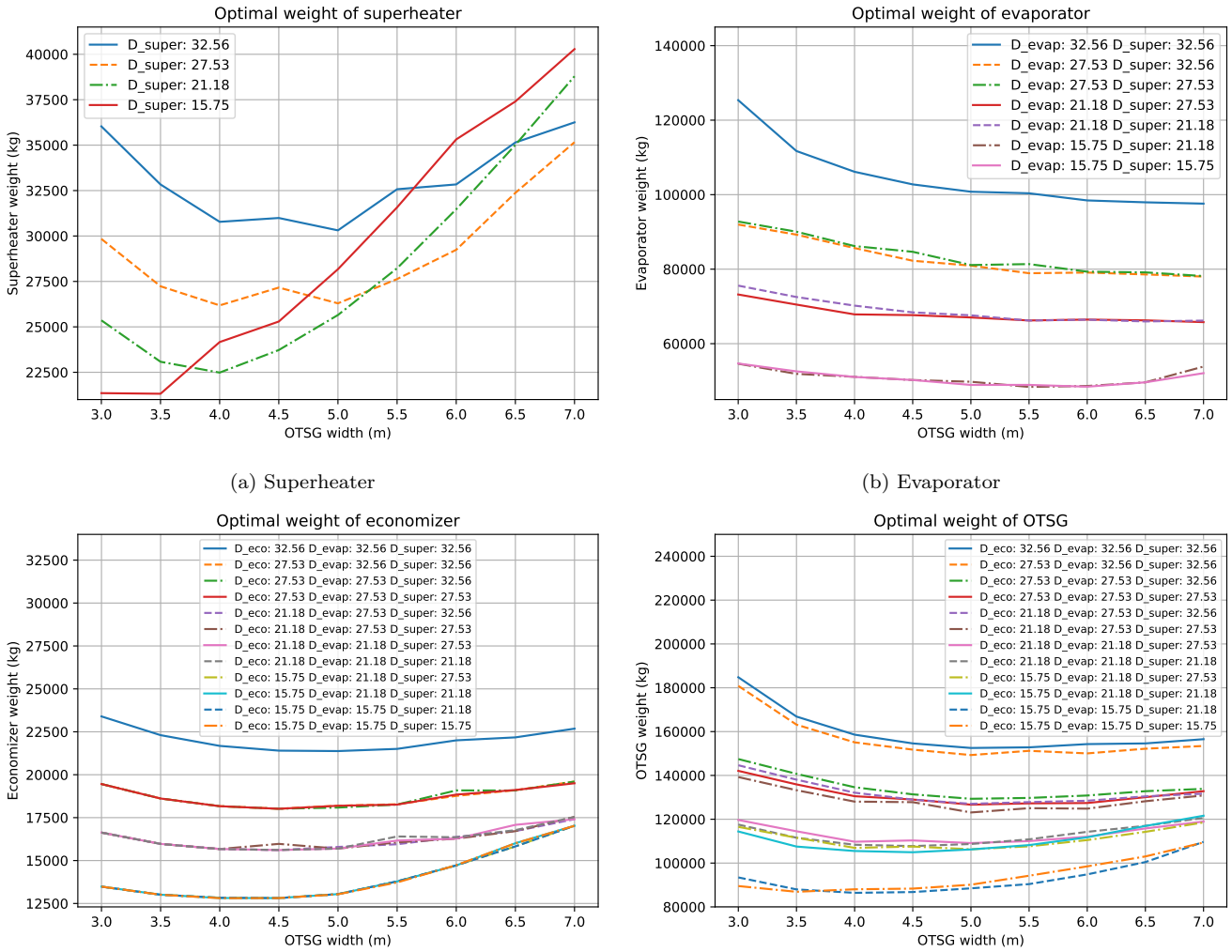

(a) Superheater

(b) Evaporator

(c) Economizer

(d) Total OTSG

Fig. 6. Weight of the optimal design of the three different cores of the OTSG as well as the total weight of the OTSG for varying widths and diameter combinations given in Table 4. Repeating combinations in the superheater and evaporator are not included to ease readability. The minimum weight is reduced with tube diameter and the evaporator is the heaviest and has the biggest reductions.

Table 5. Time for each three-core design to reach 1% and 0.1% of the final steady state value of the water at superheater outlet when changing the gas turbine load from 90% to 50%. The response time is reduced for smaller tube diameters, and the evaporator has the biggest impact.

Superheater [mm]	Evaporator [mm]	Economizer [mm]	Time for ±1% [s]	Time for ±0.1% [s]
32.56	32.56	32.56	9521	19995
32.56	32.56	27.53	9563	19935
32.56	27.53	27.53	7657	16072
27.53	27.53	27.53	7698	16205
32.56	27.53	21.18	7596	15873
27.53	27.53	21.18	7517	15824
27.53	21.18	21.18	6484	13672
21.18	21.18	21.18	6657	14118
27.53	21.18	15.75	6393	13462
21.18	21.18	15.75	6280	13160
21.18	15.75	15.75	5079	10992
15.75	15.75	15.75	5114	10805

REFERENCES

Bennett, D.L. and Chen, J.C. (1980). Forced convective boiling in vertical tubes for saturated pure components and binary mixtures. *AIChE Journal*, 26(3), 454–461. doi:10.1002/aic.690260317.

Deng, H., Skaugen, G., Næss, E., Zhang, M., and Øiseth, O.A. (2021). A novel methodology for design optimization of heat recovery steam generators with flow-induced vibration analysis. *Energy*, 226, 120325. doi:10.1016/j.energy.2021.120325.

Friedel, L. (1979). Improved Friction Pressure Drop Correlation for Horizontal and Vertical Two-Phase Pipe Flow. In *European Two-Phase Flow Group Meeting*. Ispara, Italy.

Galassi, M., Davies, J., Theiler, J., Gough, B., Jungman, G., Alken, P., Booth, M., and Rossi, F. (2009). *GNU Scientific Library Reference Manual*. Network Theory Ltd., Bristol, third edition edition.

Ganapathy, V. (2002). *Industrial Boilers and Heat Recovery Steam Generators: Design, Applications, and Calculations*. CRC Press, Boca Raton. doi:10.1201/9780203910221.

Gnielinski, V. (1976). New equations for heat and mass transfer in the turbulent flow in pipes and channels. *International Chemical Engineering*, 16, 359–368.

Ledinegg, M. (1938). Instability of flow during natural and forced circulation. *Die Waerme*, 61.

Mazzetti, M.J., Hagen, B.A.L., Skaugen, G., Lindqvist, K., Lundberg, S., and Kristensen, O.A. (2021). Achieving 50% weight reduction of offshore steam bottoming cycles. *Energy*, 230, 120634. doi:10.1016/j.energy.2021.120634.

Mazzetti, M.J., Ladam, Y., Walnum, H.T., Hagen, B.L., Skaugen, G., and Nekså, P. (2014). Flexible Combined Heat and Power Systems for Offshore Oil and Gas Facilities With CO2 Bottoming Cycles. In *ASME 2014 Power Conference*. American Society of Mechanical Engineers Digital Collection. doi:10.1115/POWER2014-32169.

Montañés, R.M., Hagen, B., Deng, H., Skaugen, G., Morin, N., Andersen, M., and J. Mazzetti, M. (2023). Design optimization of compact gas turbine and steam combined cycles for combined heat and power production in a FPSO system–A case study. *Energy*, 282, 128401. doi:10.1016/j.energy.2023.128401.

Montañés, R.M., Skaugen, G., Hagen, B., and Rohde, D. (2021). Compact Steam Bottoming Cycles: Minimum Weight Design Optimization and Transient Response of Once-Through Steam Generators. *Frontiers in Energy Research*, 9. doi:10.3389/fenrg.2021.687248.

Motamed, M.A. and Nord, L.O. (2022). Development of a simulation tool for design and off-design performance assessment of offshore combined heat and power cycles. In *63rd International Conference of Scandinavian Simulation Society, SIMS 2022, Trondheim, Norway, September 20-21, 2022*, 1–8. doi:10.3384/ecp192001.

Nord, L.O. and Bolland, O. (2012). Steam bottoming cycles offshore - Challenges and possibilities. *Journal of Power Technologies*, 92(3), 201–207.

Norwegian Petroleum Directorate (2023). Emissions to air. https://www.norskpetroleum.no/en/environment-and-technology/emissions-to-air/.

Pierobon, L., Benato, A., Scolari, E., Haglind, F., and Stoppato, A. (2014). Waste heat recovery technologies for offshore platforms. *Applied Energy*, 136, 228–241. doi:10.1016/j.apenergy.2014.08.109.

Pierobon, L. and Haglind, F. (2014). Design and optimization of air bottoming cycles for waste heat recovery in off-shore platforms. *Applied Energy*, 118, 156–165. doi:10.1016/j.apenergy.2013.12.026.

Schittkowski, K. (1986). NLPQL: A fortran subroutine solving constrained nonlinear programming problems. *Annals of Operations Research*, 5(2), 485–500. doi:10.1007/BF02022087.

Skaugen, G., Kolsaker, K., Walnum, H.T., and Wilhelmsen, Ø. (2013). A flexible and robust modelling framework for multi-stream heat exchangers. *Computers & Chemical Engineering*, 49, 95–104. doi:10.1016/j.compchemeng.2012.10.006.

Skaugen, G., Walnum, H.T., Hagen, B.A.L., Clos, D.P., Mazzetti, M.J., and Nekså, P. (2014). Design and Optimization of Waste Heat Recovery Unit Using Carbon Dioxide as Cooling Fluid. In *ASME 2014 Power Conference*. American Society of Mechanical Engineers, Baltimore, Maryland, USA. doi:10.1115/POWER2014-32165.

STEELTUBE (2021). Dimensions and Weights of Seamless Tubes According to Standard ANSI/ASME B36.10M.

Wagner, W. and Pruß, A. (2002). The IAPWS formulation 1995 for the thermodynamic properties of ordinary water substance for general and scientific use. *Journal of Physical and Chemical Reference Data*, 31, 387.

Walnum, H.T., Nekså, P., Nord, L.O., and Andresen, T. (2013). Modelling and simulation of CO2 (carbon dioxide) bottoming cycles for offshore oil and gas installations at design and off-design conditions. *Energy*, 59, 513–520. doi:10.1016/j.energy.2013.06.071.

Wilhelmsen, Ø., Aasen, A., Skaugen, G., Aursand, P., Austegard, A., Aursand, E., Gjennestad, M.A., Lund, H., Linga, G., and Hammer, M. (2017). Thermodynamic Modeling with Equations of State: Present Challenges with Established Methods. *Industrial & Engineering Chemistry Research*, 56(13), 3503–3515. doi:10.1021/acs.iecr.7b00317.